THE JOURNAL OF PHYSICAL CHEMISTRY B

Article

pubs.acs.org/JPCB

Molecular Insight into the Ligand−IgG Interactions for 4-Mercaptoethyl-pyridine Based Hydrophobic Charge-Induction Chromatography

Dong-Qiang Lin,* Hong-Fei Tong, Hong-Yin Wang, and Shan-Jing Yao

State Key Laboratory of Chemical Engineering, Department of Chemical and Biological Engineering, Zhejiang University, Hangzhou 310027, China

Supporting Information

ABSTRACT: Hydrophobic charge-induction chromatography (HCIC) with 4-mercaptoethyl-pyridine (MEP) as the ligand is a novel technology for antibody purification. In the present work, the molecular simulation methods were used to investigate the interactions between MEP ligand and Fc fragment of IgG (Fc-A). Six ligands with different structures of spacer arm were studied with molecular docking and dynamics simulation at neutral and acidic pH. The binding modes and the interaction energies were analyzed. The results indicated that all ligands tested could bind into the selected pocket on the C_{H2} domain of Fc-A at neutral pH. The pyridine ring on the top of MEP ligands acts as a major role to provide the hydrophobic association and hydrogen bond for the ligand−IgG binding; meanwhile, the sulfone group on the spacer arm might form the additional hydrogen bond and enhance the binding of ligand onto the surface of IgG. The replacements of thioether sulfur atom on the spacer arm with either nitrogen or oxygen atom seem to have little influence on the binding. The influences of pH on the ligand−IgG interactions were also studied with the molecular dynamics simulation. It was found that MEP ligands would departed from the surface of Fc-A at low pH due to the electrostatic repulsion. The ligands with a sulfone group on the spacer arm would weaken the electrostatic repulsion and need more acidic conditions for the departing of ligand. The molecular simulation results were in agreement with some experimental observations, which would be useful to elucidate the molecular mechanism of HCIC and design a novel ligand to improve the efficiency of antibody separation.

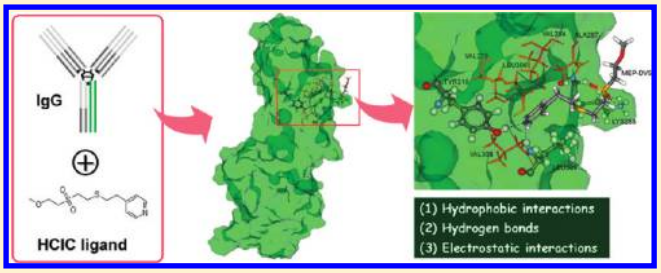

1. INTRODUCTION

Monoclonal antibodies (mAbs) and related molecules constitute the majority of biopharmaceutical products currently.[1,2] Because of the highly improved upstream productivity of mammalian cell culture over the past few years, the downstream processes have now become a key bottleneck in the production of antibodies.[3] In many cases, Protein A affinity chromatography has been adopted as a platform approach for the capture of an antibody with high specificity. However, there are still some limitations on the Protein A capture, such as high cost, relatively low reusability of Protein A resin, ligand leaching, antibody aggregation at low pH elution conditions, and some difficulties on the Clean-In-Place (CIP).[4−7] In order to improve the process of antibody production, the alternatives to Protein A capture have become an area of active investigation.[4,5,8]

In 1998, Burton and Harding[9] introduced a new type of chromatographic technology, hydrophobic charge-induction chromatography (HCIC), which is based on the pH-dependent behavior of dual-mode ionizable ligands that combine the hydrophobic and electrostatic interactions together. One of the typical ligands for HCIC is 4-mercaptoethyl-pyridine (MEP) with the pK_a of 4.8, which shows a noncharge at neutral conditions but becomes positively charged at low pH. HCIC with MEP ligand has been used as an effective method for the separation of IgG from a variety of feedstocks.[10] For HCIC, high dynamic binding capacity was often reported, which was independent of the ionic strength over a broad range. Normally, efficient elution can be achieved under relatively mild conditions at pH 4.0 due to the electrostatic repulsion between MEP ligand and IgG.[11,12] The performances of HCIC and Protein A chromatography have also been compared, and the results indicated that HCIC could provide efficient isolation and purification of antibodies from both protein-free cell culture supernatants and the clarified/concentrated milk of transgenic goats.[13] In general, HCIC represents a cost-effective alternative to Protein A chromatography for the purification of antibody.

On the basis of the concept of HCIC, the adsorption is primarily due to the hydrophobic interactions between protein and the hydrophobic groups of the ligand, and the desorption at acidic conditions is mainly caused by the electrostatic repulsion with the charge induction of ligand and protein.[10−13] Some studies indicated that MEP ligand prefers to interact with the hydrophobic regions of IgG, which are mostly present on

Received: July 17, 2011
Revised: December 6, 2011
Published: January 3, 2012

dx.doi.org/10.1021/jp206817b | J. Phys. Chem. B 2012, 116, 1393−1400

the Fc fragment.[10,12] Although the ligand−protein interaction modes mentioned above have been used conceptually to interpret the performance of HCIC, it is still quite limited on the understanding of the molecular mechanism of hydrophobic binding and electrostatic-repulsion elution. With the help of molecular simulation tools,[14−16] it is now possible to investigate the nature of ligand−protein interactions from a molecular view. Cavallotti et al.[17−19] studied the ligand−protein interactions in affinity chromatography for antibody purification, and the IgG−ligand−substrate complex system represented by the full-atomic model was constructed using PAM, A2P, and Protein A as the ligands. Zhang et al.[20−23] established the 46-bead β-barrel coarse-grained model to investigate the conformational transition of protein and the effect of composition, density, and homogeneity of ligands on HCIC. In our earlier work,[24] the interactions between a model of MEP ligand ($-O-CH_2-CH_2-CH_2-S-CH_2-CH_2-C_5H_4N$, MEP−AB) and the Fc fragment of IgG were studied with molecular simulation. The results indicated that MEP−AB ligand can bind stably on the pocket around TYR319 and LEU309 of the Fc chain of IgG at neutral conditions and departs quickly at pH 4.0.

To better understand the roles of ligand structure on the binding in HCIC, more details on the ligand−protein interactions should be investigated. Normally, the HCIC ligands can be coupled onto the matrix by two activation reagents, allyl bromide (AB) or divinyl sulfone (DVS).[10,25,26] When MEP is coupled after the activation with DVS, the ligand becomes as $-O-CH_2-CH_2-SO_2-CH_2-CH_2-S-CH_2-CH_2-C_5H_4N$ (MEP−DVS), which has an additional sulfone group on the spacer arm. Some results in the literature indicated that the differences on the spacer arm of the ligand would influence the adsorption properties of the antibody.[10,26] It was also found that both the sulfur atom of sulfone and thioether group contribute in the formation of so-called thiophilic interaction.[10,27] Therefore, in the present work, six ligands with MEP as the model functional group will be established, and the effects of spacer arm (especially for sulfur atom) on the ligand−IgG binding will be studied in detail with the aids of molecular docking and dynamics simulations. The interaction energies and the influence of pH will be analyzed to reveal the separation mechanism of HCIC.

2. MOLECULAR MODEL AND SIMULATION METHODS

The molecular simulation is implemented with the software platform of Discovery Studio (DS, Accelrys Inc., San Diego, USA), and the working scheme is shown in Figure 1. The PDB files containing the molecular structure information of protein can be obtained from the public resource of Protein Data Bank (PDB, www.rcsb.org/pdb/), and the ligand molecules are constructed with DS. First, the ligand is docked onto the surface of the protein, and the potential binding mode of the ligand−protein complex would be obtained. Second, the ligand−protein binding complex is put into the environment of molecular dynamics (MD) simulation to evaluate the binding mode at neutral pH. Third, the system is changed to acidic pH conditions, and the departing mode of the ligand from the surface of the protein can be evaluated with MD simulation. Finally, the ligand−protein molecular interactions and the interaction energies would be analyzed, and the mechanism of adsorption and desorption of HCIC can be discussed.

2.1. Molecular Models. The molecular structure of the Fc fragment of IgG was obtained from the Protein Data Bank (PDB) with the ID code of 1FC1.[28] 1FC1 consists of twin $C_{H2}-C_{H3}$ domains of IgG1, which contain the identical amino acid sequence and are similar in the 3D structure. Therefore, only chain A of

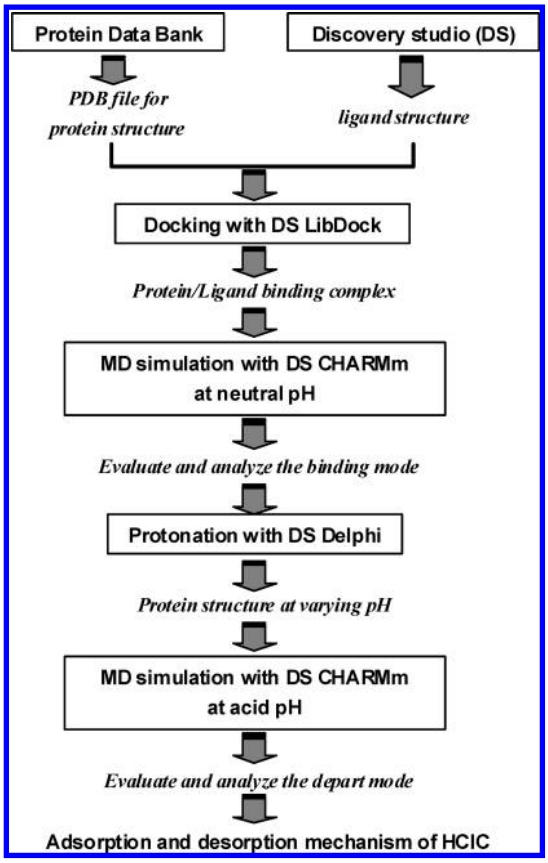

Figure 1. Scheme of molecular simulation procedure.

1FC1 (defined as Fc-A) was considered here for further study to reduce the computational expense. The molecular surface and hydrophobic properties on the surface of Fc-A are shown in Figure 2. For the molecular simulation of Fc-A, CHARMM22 force field parameters were used in the present work.

The HCIC ligands tested are shown in Figure 3. In the present work, the structure differences of ligand on the ligand−protein interactions are focused, so the matrix is represented by a methyl group to simplify the molecular model. As we know, this is just an approximation on the ligand, and in real use, the ligand is immobilized on the matrix support for the chromatographic separation. Normally, MEP ligands can be coupled to the matrix with the activation of allyl bromide (AB) or divinyl sulfone (DVS), respectively, for MEP−AB and MEP−DVS in Figure 3. For MEP−DVS, there is an additional sulfone group on the spacer arm. Furthermore, some derivatives in which the sulfur atom of a thioether group is replaced by either an oxygen or nitrogen atom are named as MEP−AB_S−O, MEP−AB_S−N, MEP−DVS_S−O and MEP−DVS_S−N, respectively. All six ligand molecules were constructed with DS, and the force field parameters are provided in Table S1 of the Supporting Information.

2.2. Molecule Ionization and Electrostatic Potential Analysis. The ionization status of Fc-A at different pH conditions was predicted by the protocol of Calculate Protein Ionization and Residue pK_a provided by DS, The calculations of the protein ionization and residue pK_as in Discovery Studio are based on a fast and accurate computational approach to pH-dependent electrostatic effects in protein molecules. The protocol also includes a CHARMM-based algorithm to construct and optimize the hydrogen coordinates at a given pH. The detailed description of the methods used can be found in the ref 29.

dx.doi.org/10.1021/jp206817b | J. Phys. Chem. B 2012, 116, 1393−1400

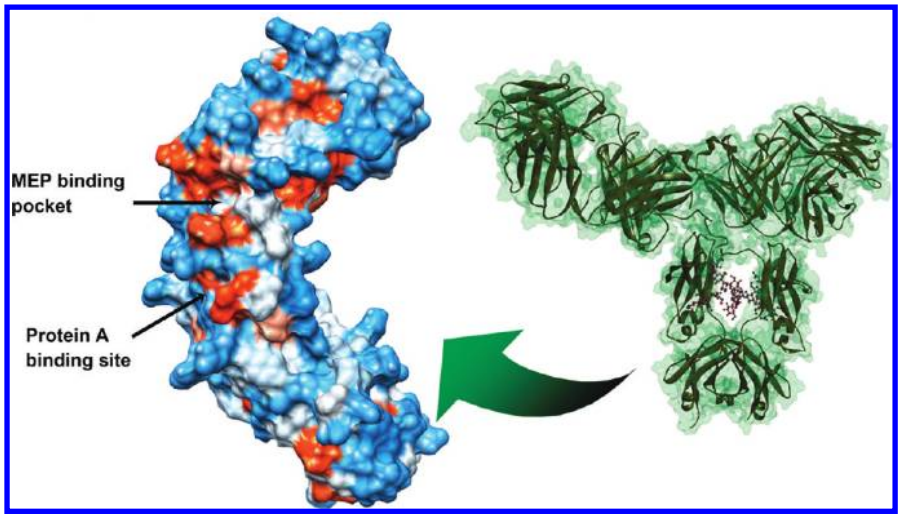

Figure 2. Molecular surface of Fc-A domains of IgG1 (PDB ID: 1FC1). The protein surface is colored by the hydrophobicity of the amino acid with the software of UCSF-Chimera,[36] ranging from dodger blue for the most polar residues to orange-red for the most hydrophobic residues.

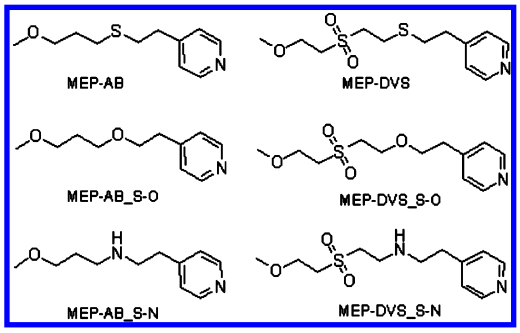

Figure 3. Molecular structure of the HCIC ligands tested.

For MEP ligand testing, the positive-charged status was achieved by simply adding a hydrogen atom on nitrogen and changing the net charge to +1.

The electrostatic potentials of protein and ligand at different pHs were calculated using the well-known DelPhi program by the protocol of Electrostatic Potential provided by DS.[30,31] The solvent accessible surface was created with the probe radius of 1.4 Å.

2.3. Molecular Docking. On the basis of our previous work,[24] six possible binding sites were found on the surface of Fc-A for MEP ligand. The distribution of possible binding sites on Fc-A is shown in Figure S1 and some interaction information can be found in Table S2 in the Supporting Information. After the evaluation of molecular docking and dynamic simulation, a pocket around TYR319 and LEU309 (as shown in Figure 2) was identified as the most possible binding site for MEP ligand on Fc-A, which is a little above the consensus binding site (hinge region between C_{H2} and C_{H3} domains) for Protein A identified by Delano et al.[32] This binding pocket for MEP ligand is located at the C_{H2} domain of the Fc fragment of IgG and consists of several hydrophobic residues such as VAL279, VAL284, ALA287, LEU306, VAL308, and LEU309. Therefore, in the present work, this site was considered as the candidate binding pocket for the molecular docking with the LibDock module[33] in DS to find out possible binding modes between ligand and Fc-A.

The binding energies (BE) between the docked ligand and Fc-A were estimated using the protocol of Calculate Binding Energies provided by DS.[34] The implicit solvent mode of Poisson–Boltzmann with nonpolar Surface Area (PBSA) was used, and the BE is calculated as follows:

$$\text{Energy}_{\text{binding}} = \text{Energy}_{\text{complex}} - \text{Energy}_{\text{ligand}} - \text{Energy}_{\text{receptor}}$$

After the docking, only the conformations with the head (pyridine ring) of MEP ligand embedded into the binding pocket were considered as the rational modes. Then, the potential binding modes were evaluated, and those with low BE were selected to construct the complex of ligand and Fc-A for the MD simulation.

2.4. Molecular Dynamics Simulation. *2.4.1. Simulation at Neutral Conditions.* After the docking, the potential binding complex of ligand and Fc-A was obtained and evaluated by the MD simulations using the CHARMM module provided by DS. The MD simulations were done as follows. (1) Solvation: solvate the complex structure in an orthorhombic box with periodic boundary conditions (PBC), leaving a minimum distance of 7 Å between the complex and the edge of the box. TIP3P water was used. Na^+ and Cl^- counterions were added to neutralize the system. (2) Minimization: first, impose Harmonic Restraint on the complex with the Force Constant of 100, perform 500 cycles with the Steepest Descent algorithm, and then perform 1000 cycles with the Conjugate Gradient algorithm to remove any possible unfavorable contact between solvent and solute. Second, remove the Harmonic Restraint, perform 500 cycles with the Steepest Descent algorithm, and then perform 1000 cycles with the Conjugate Gradient algorithm. (3) Heating: raise the temperature of system from 50 to 300 K with the time step of 1 fs in 20 ps. In this phase, the Harmonic Restraint with the Force Constant of 10 was imposed on the complex to avoid wild structural fluctuation. (4) Equilibration: run for 100 ps with the time step of 1 fs at constant pressure to allow the water density to relax. The Force Constant of Harmonic Restraint was diminished to 0.01. (5) Production: run for 4 ns with the time step of 2 fs at constant pressure and temperature of 300 K. In this phase, the SHAKE algorithm was used to restrain all the covalent bonds involving hydrogen.[35]

In order to avoid the relative bending of the C_{H2} and C_{H3} domains during the simulations and meanwhile keep some degrees of freedom of the residues, a weak Harmonic Restraint

dx.doi.org/10.1021/jp206817b | J. Phys. Chem. B 2012, 116, 1393–1400

with the Force Constant of 0.01 was imposed on the backbone of Fc-A. Snapshots were collected every 2 ps and used for successive analysis. In all MD simulations, the nonbonded cutoff was set as 14 Å and long-range electrostatic interactions were evaluated using the Particle Mesh Ewald (PME) method.

2.4.2. Simulation at Acidic Conditions. The conformation of the ligand−Fc complex at the end of a 2 ns simulation was taken, and the Fc-A molecule was, respectively, protonated at pH 4.0 and 3.0 by the protocol of Calculate Protein Ionization and Residue pK_a provided by DS as mentioned above. The MEP ligand was protonated by adding a hydrogen atom to the nitrogen atom. New ligand−Fc complexes were used to represent the status of pH 4.0 or pH 3.0, respectively, then ran the MD simulations following the steps described above.

2.4.3. Interaction Energy and Simulation Analysis. The total interaction energy (TIE) between the ligand and Fc-A, defined as the sum of electrostatic interaction energy (EIE) and van der Waals interaction energy (VIE), was calculated by the CHARMM-based protocol of Calculates Interaction Energy provided by DS. The Implicit Distance-Dependent Dielectrics as the dielectric model was used.

The simulation results were also analyzed using the UCSF-Chimera[36] and VMD 1.8.7.[37]

3. RESULTS AND DISCUSSION

3.1. Molecular Docking. On the basis of our previous work,[24] the pocket located on the C_{H2} domain of the Fc fragment of IgG was selected as the potential binding site for molecular docking as shown in Figure 2. As expected, all six MEP ligands tested were successfully docked into the candidate pocket. Tens of binding modes (docked conformations) for each ligand were obtained, and four rational binding modes of each ligand with the lowest BE were selected to construct the potential binding complex of ligand and Fc-A. For example, the selected binding modes of MEP−DVS are shown in Figure 4.

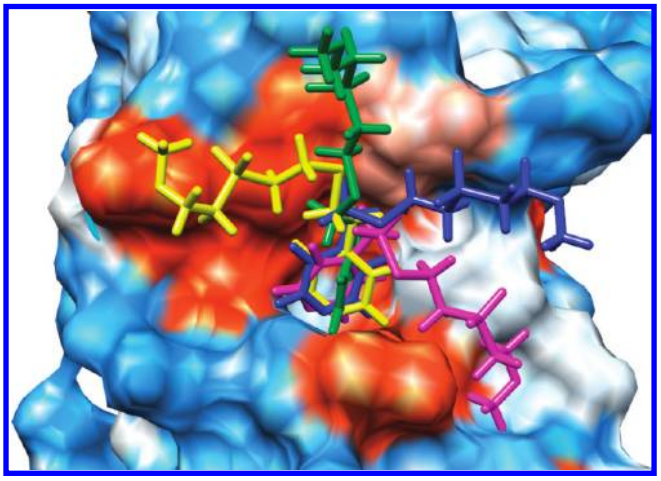

Figure 4. Four binding modes of MEP−DVS on the binding pocket of Fc-A. Each conformation of MEP−DVS is shown by stick and colored differently. The protein surface is colored by the hydrophobicity of the amino acid with the software of UCSF-Chimera,[36] ranging from dodger blue for the most polar residues to orange-red for the most hydrophobic residues.

It can be found that the pyridine rings of the MEP group were embedded totally into the target pocket. The amino acid residues surrounding the MEP ligands within the distance of 3 Å are VAL279, VAL284, ALA287, LEU306, VAL308, LEU309, ASN312, LYS317, and TRY319, and most of them are hydrophobic residues, such as VAL, LEU, and ALA. It could be inferred that the hydrophobic interactions have an important role on the binding of the MEP ligand to the surface of IgG.

3.2. Molecular Dynamic Simulation at Neutral pH. After the docking, the ligand−Fc-A complex was obtained and used as the initial structure for subsequent MD simulations to evaluate the binding possibility and stability of the complex. Several important factors are monitored during the simulations, including (1) the root-mean-square deviation (rmsd) of the ligand relative to its initial structure; (2) the interaction energies between the ligand and Fc-A; and (3) the hydrogen bond formed between the ligand and Fc-A.

3.2.1. Influence of Spacer Arm of Ligand. Two ligands, MEP−AB and MEP−DVS, were used to investigate the influence of spacer arm difference on the binding effects. The results indicated that both ligands could bind on the selected site of IgG during 4 ns simulation. The rmsd values of the ligands were quite small (no more than 1.0 nm) for all simulation periods as in our previous work.[24] The TIE, together with corresponding VIE and EIE between the ligand and Fc-A during the simulation, was averaged on a time span of 0.1 ns and shown in Figure 5. It can be found that the values of the

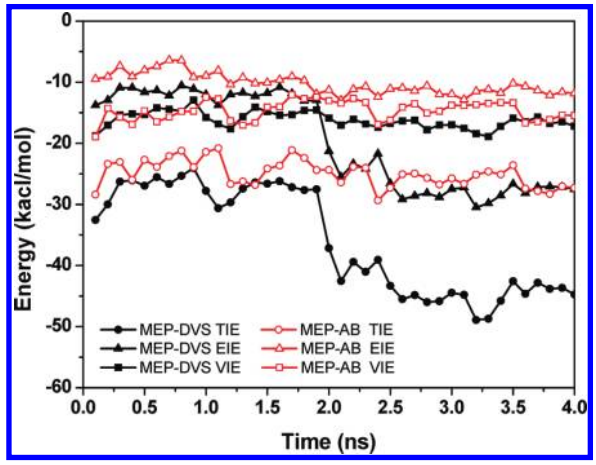

Figure 5. TIE, EIE, and VIE between the ligand and Fc-A during the simulation averaged on the time span of 0.1 ns.

VIE and EIE are of the same order of magnitude, which means that both polar and nonpolar interactions contributed to the binding of MEP ligand onto the surface of IgG.

It is necessary to analyze the interaction energies in detail to find some differences between MEP−AB and MEP−DVS. Comparing the VIE term of MEP−DVS with MEP−AB, it can be seen that the values of VIE show no essential difference during a 4 ns simulation. The VIE reflects the contributions of nonpolar interactions in the binding, which are mainly caused by the interactions between the pyridine ring of MEP and hydrophobic residues around the binding pocket. MEP−AB and MEP−DVS ligands have the same MEP functional group, so two ligands show similar VIE values to Fc-A. However, there are some differences on the ELEs of MEP−AB and MEP−DVS. The values of EIE were almost the same for the first 2 ns, but significantly declined at the last 2 ns for MEP−DVS. The analysis of trajectory of MEP−DVS simulation revealed that it was due to the formation of a hydrogen bond between the oxygen atom of sulfone and LYS288 of Fc-A as shown in Figure 6.

dx.doi.org/10.1021/jp206817b | J. Phys. Chem. B 2012, 116, 1393−1400

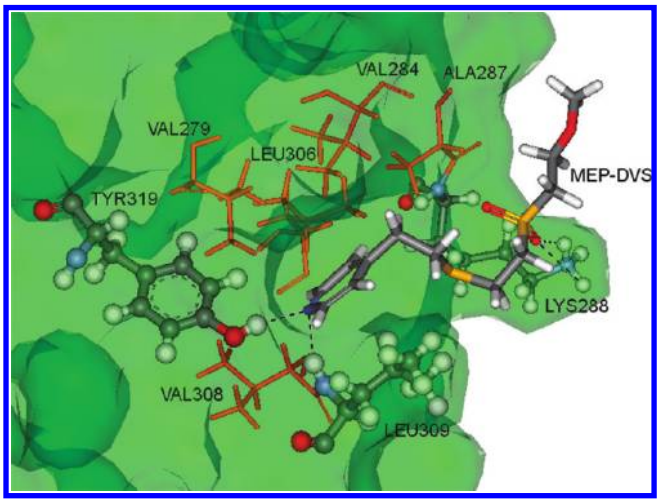

Figure 6. Simulation snapshot of the binding of MEP−DVS on the surface of Fc-A. The hydrogen bonds between MEP−DVS ligand and TYR319 and LEU309 as well as LYS288 of Fc-A around the hydrophobic binding site are marked with a black dotted line. MEP is shown by the thick stick, while TYR319, LEU309, and LYS288 are shown by the thin ball and stick, and the hydrophobic amino acids surrounding MEP−DVS within 3 Å (except LEU309) are shown by the orange thin stick. The surface of the protein is displayed by a green transparent surface.

During the first 2 ns, the distance between sulfone and LYS288 was too far to form any hydrogen bond. As time evolved, two parts approached each other, and at about 2 ns, they were close enough to form the hydrogen bonds. Once the hydrogen bonds were formed, the binding of MEP−DVS to Fc-A was enhanced, and the values of EIE became more negative. Besides the hydrogen bond between sulfone and LYS288, two more hydrogen bonds also existed between the nitrogen atom of pyridine and TYR319 or LEU309 as in the case of the MEP−AB ligand (see Figure 6).

To further evaluate the contributions of two parts (MEP group and DVS spacer arm) of the MEP−DVS ligand in the binding, the interaction energies between each part and Fc-A were calculated separately and shown in Figure 7. It could be

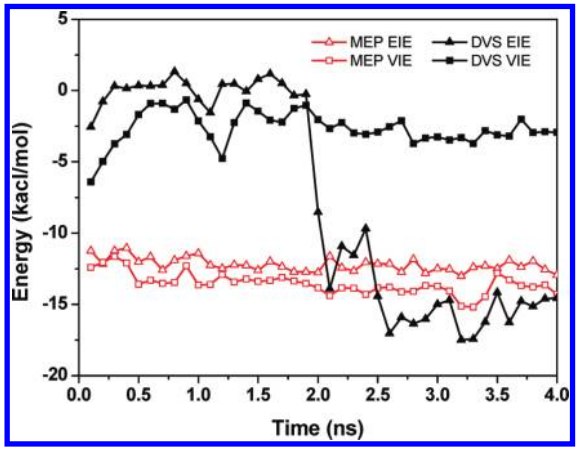

Figure 7. Comparison of the contributions of the MEP group and spacer arm (DVS part) in the calculated interaction energies for MEP−DVS binding.

clearly found that the contributions of two parts were significantly different. The relatively stable values of VIE (∼−13.5 kcal/mol) and EIE (∼−12.0 kcal/mol) reflected the nonpolar association and hydrogen bond between the MEP part and Fc-A. Compared to the MEP part, the VIE values of the DVS part were near zero (about −3.0 kcal/mol), which meant that the contribution of the DVS part on the nonpolar interactions was quite low. However, the EIE values of the DVS part changed evidently during the simulation, and the trend was similar to the whole ligand of MEP−DVS as shown in Figure 5. The EIE values of the DVS part were kept at almost zero in the first 2 ns, and then decreased and stabilized around −15 kcal/mol in the next 2 ns. As mentioned above, it was caused by the formation of an additional hydrogen bond between sulfone and LYS288. The results demonstrated further that the pyridine ring on the top of the MEP−DVS ligand acts as a major role to provide the hydrophobic association and hydrogen bond together; meanwhile, the sulfone group on the spacer arm could form the additional hydrogen bond and enhance the binding of the ligand onto the surface of IgG. This observation is in agreement with that stated by Boschetti,[10] when MEP is immobilized after activation of the matrix with divinyl sulfone, the ligand showed an increase in the binding capacity for IgG and a reduction of the dissociation constant value.

3.2.2. Influence of Thioether Sulfur of Ligand. Four ligands, MEP−AB_S−O, MEP−AB_S−N, MEP−DVS_S−O, and MEP−DVS_S−N, were tested to evaluate the role of the sulfur atom of the thioether group in the spacer arm on the binding of the MEP ligand. When the sulfur atom of the thioether group was replaced by either an oxygen atom or nitrogen atom, the simulation results showed no significant difference on the binding of the ligand. Four ligands tested could bind stably on the selected binding pocket during the simulation, and the existence of hydrogen bonds were almost the same as the case of MEP−AB and MEP−DVS. Furthermore, the calculated TIE, EIE, and VIE were also similar to those of MEP−AB and MEP−DVS, respectively, as shown in Figures S2 and S3 of the Supporting Information. It seemed that the simulation results could not verify the influences of thioether sulfur on the binding of MEP ligands. Boschetti[10] stated that when the sulfur atom was replaced by either a nitrogen atom or an oxygen atom, while maintaining the pyridine ring in place, the binding capacity for IgG in physiological conditions would be much lower compared to a sulfur-containing ligand. However, there was no experimental data published to confirm that conclusion. Porath and Hutchens[38,39] reported that the ligands for thiophilic adsorption of IgG could be generally represented as $-SO_2CH_2CH_2X-$, where X was first a thioether but might also be N and O or possibly any atom with at least one lone electron pair. It was reported that the sulfone group and thioether sulfur (or other electron donor like N and O) cooperate to form some kind of ring structure by transfer of electrons or protons between the ligand site and the corresponding countersite on the protein.[38] Furthermore, Berna et al.[40] proposed that the name of thiophilic adsorption chromatography (TAC) should be updated to electron donor−acceptor chromatography (EDAC) as similar protein selectivity is demonstrated for electron donor−acceptor ligand devoid of sulfur atoms. Therefore, due to the contradiction of results reported, it is still difficult to conclude if the thioether sulfur plays an important role on the ligand−IgG binding. More experimental and theoretical studies are needed.

3.3. Molecular Dynamics Simulation at Acidic Conditions. In order to evaluate the influence of pH on the ligand−IgG binding and reveal the mechanism of charge-induced repulsion for HCIC, the ligand−IgG binding complex was challenged for acidic conditions. The conformation of Fc-A at the end of the above MD simulation was taken and protonated at pH 4.0 and 3.0, respectively. The net charges of

dx.doi.org/10.1021/jp206817b | J. Phys. Chem. B 2012, 116, 1393−1400

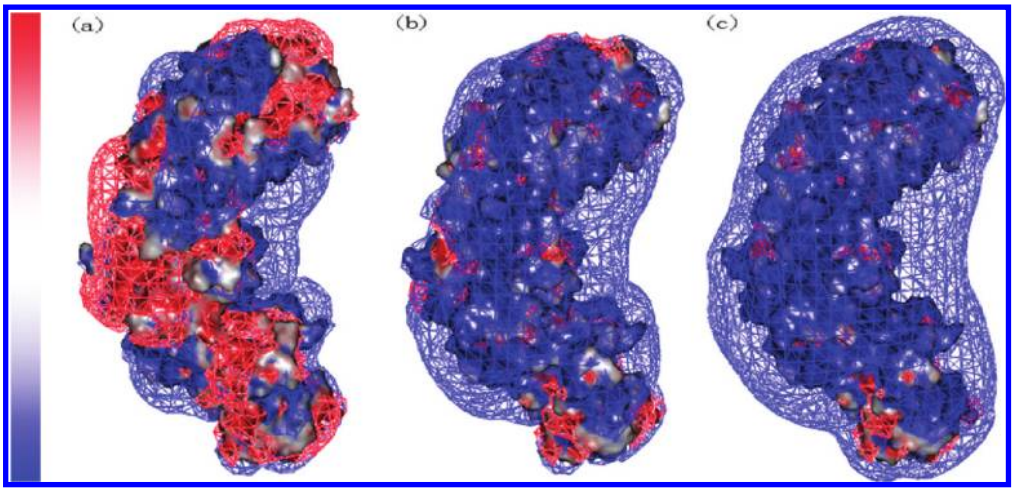

Figure 8. Solvent accessible surface and isopotential surface of Fc-A at pH 7.0 (a), pH 4.0 (b), and pH 3.0 (c). The solvent surface is colored according to the electrostatic potential, deep red for −5 kT/e and deep blue for +5 kT/e. The isopotential surface is displayed in triangle mesh, red for −1 kT/e and blue for +1 kT/e.

Fc-A at pH 4.0 and 3.0 are +16 and +23, respectively, in contrast with +4 at neutral pH. The positively charged residues around the binding pocket at low pH include HIS285, LYS288, LYS290, HIS310, LYS317, and LYS320. The solvent accessible surface and isopotential surface of Fc-A at different pHs are shown in Figure 8. It can be found that the decrease of pH from 7.0 to 4.0 evidently influences the ionization of Fc-A, resulting in the obviously increasing area of surface that corresponds to positive electrostatic potential and largely decreasing area of surface that corresponds to negative electrostatic potential. When the pH is dropped to 3.0, the surface of Fc-A becomes more positively charged and has stronger positive electrostatic potential than that at pH 4.0. This would certainly influence the interactions between MEP ligands and Fc-A at acidic conditions, which will be discussed in the next section.

As reported in our earlier works,[24] during 1 ns MD simulation MEP−AB ligand could depart quickly from the binding pocket when the pH lowers to 4.0. The rmsds of the MEP−AB ligand at pH 4.0 and pH 7.0 have been published previously,[24] and the distance between the N atom of MEP−AB and residue LEU 309 are shown in Figure S4 of the Supporting Information. Figure 9 shows the EIE and VIE between MEP−AB and Fc-A during the simulation. It can be seen that the EIE could keep relatively stable at pH 7.0, fluctuating around −12.0 kcal/mol. However, when the pH lowered to 4.0, the values of EIE turned positive immediately at the beginning of the simulation, which means there was electrostatic repulsion between the MEP−AB ligand and Fc-A. The EIE decreased to near zero in 0.1 ns, which could be explained by the increasing distance between MEP−AB and the binding pocket on Fc-A. As shown in Figure 9b, the VIE also kept relatively stable at pH 7.0, which meant that strong hydrophobic interactions always existed between the MEP−AB and Fc-A at neutral conditions. At pH 4.0, the VIE approached zero after 0.3 ns simulation, which represented that there were no molecular interactions between the ligand and protein due to the long distance of the two molecules.

As expected, the case of the MEP−DVS ligand was a little differentfrom MEP−AB at acidic conditions. The rmsds of ligands at different pH values are shown in Figure 10. For pH 7.0, the rmsd values kept less than 1.0 nm during 2 ns simulation, which meant that MEP−DVS could be maintained on the binding pocket at neutral pH. For pH 4.0, the rmsd values kept in 1.0 nm

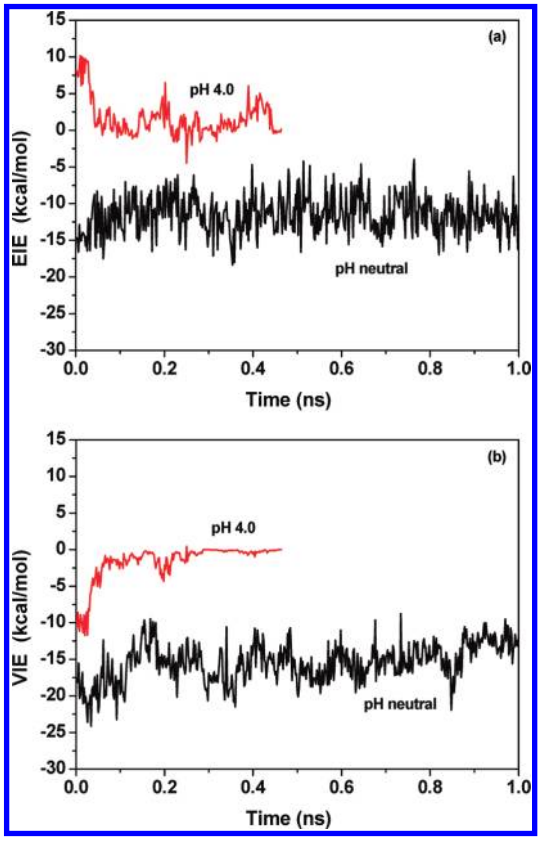

Figure 9. EIE (a) and VIE (b) between MEP−AB and Fc-A during the MD simulation at neutral pH and pH 4.0.

at the beginning for 1.2 ns, and then increased to about 2.0 nm at the end of the 2 ns simulation. By analyzing the trajectory, it could be found that the pyridine ring of the MEP−DVS ligand was gradually repulsed out of the binding pocket as time evolved, but the hydrogen bonds between sulfone and LYS288 continued to exist for about 1.2 ns. The ligand looked like it was hanging on the LYS288 by the hydrogen bonds as shown in Figure 11. At last, the hydrogen bonds were broken, and MEP−DVS departed from the surface of Fc-A. For pH 3.0, the pyridine ring of the MEP−DVS ligand moved quickly out of the binding pocket, and the MEP−DVS ligand departed from the surface of Fc-A soon at the

dx.doi.org/10.1021/jp206817b | J. Phys. Chem. B 2012, 116, 1393−1400

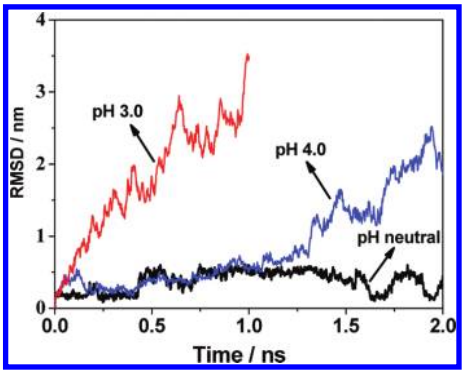

Figure 10. rmsds of MEP−DVS during the simulation at pH 7.0, 4.0, and 3.0.

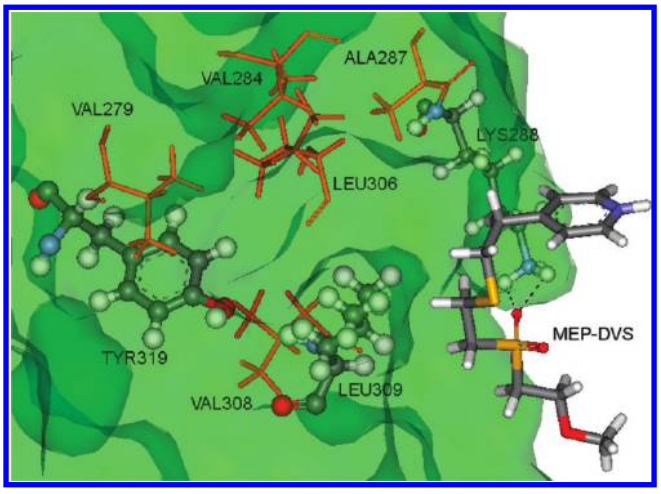

Figure 11. MEP−DVS hanging on LYS288 with the hydrogen bonds at pH 4.0. The hydrogen bonds between the MEP−DVS ligand and LYS288 of Fc-A are marked with a black dotted line. MEP is shown by the thick stick, while TYR319, LEU309, and LYS288 are shown by the thin ball and stick, and the hydrophobic amino acids surrounding MEP−DVS within 3 Å (except LEU309) are shown by the orange thin stick. The surface of the protein is displayed by a green transparent surface.

beginning of simulation, corresponding to the prompt increase of rmsd at pH 3.0 as shown in Figure 10.

The EIE and VIE between MEP−DVS and Fc-A at different pHs are shown in Figure 12. Compared to the obviously positive EIE values at pH 4.0 for the MEP−AB ligand, the EIE values in the case of the MEP−DVS ligand were always negative either at pH 4.0 or 3.0. This could be attributed to additional hydrogen bonds between the sulfone group of MEP−DVS and LYS288 on the binding pocket of Fc-A. Although the electrostatic repulsion effect existed between the positively charged pyridine ring and Fc-A, the calculated EIE values still appear to be negative. When the hydrogen bonds were broken, the EIE values trended to zero as the ligand left far away from the surface of Fc-A. As shown in Figure 12b, the VIE also kept relatively stable at pH 7.0, meaning strong hydrophobic interactions between the MEP−DSV and Fc-A. At acidic conditions, the VIE approached to zero after 1.3 ns simulation for pH 4.0 and 0.25 ns for pH 3.0, due to the long distance between MEP−DSV and Fc-A.

On the basis of the simulation results, compared with MEP−AB, the MEP−DVS ligand with one sulfone group on the spacer arm might weaken the electrostatic repulsion and need

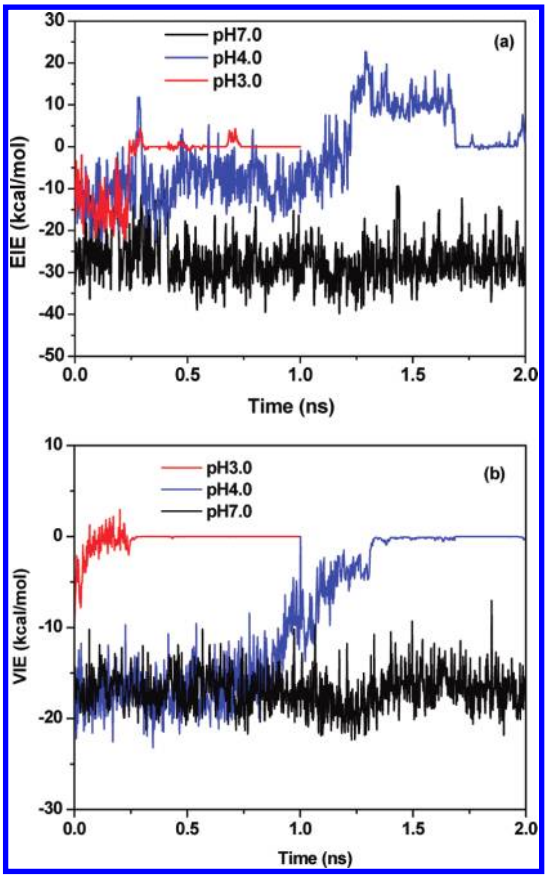

Figure 12. EIE (a) and VIE (b) between MEP−DVS and Fc-A during the MD simulation at pH 7.0, 4.0, and 3.0.

more acidic conditions for the departing of ligand, which implied that for the MEP−DVS ligand, more acidic conditions should be adopted for efficient elution of IgG.

4. CONCLUSIONS

The molecular interactions between the MEP ligand and Fc fragment of IgG (Fc-A) were investigated with molecular simulation methods at neutral and acidic pH conditions. Several MEP-based ligands were built to investigate the influences of spacer arm, including a sulfone group and thioether sulfur. The MEP−AB ligand can bind stably on the binding pocket around TYR319 and LEU309 of Fc-A at neutral pH and departs quickly when pH lowers to 4.0. The MEP−DVS ligand with a sulfone group on the spacer arm can also bind onto the same binding pocket with stronger interactions due to an additional hydrogen bond between sulfone and residue LYS288. The EIE values of MEP−DVS showed evidently higher than those of MEP−AB, mainly due to the additional hydrogen bond. The simulation results indicated that during binding, the pyridine ring on the top of the MEP ligand acts as a major role to provide the hydrophobic association and hydrogen bond together; meanwhile, the sulfone group on the spacer arm could form the additional hydrogen bond and enhance the binding of the ligand onto the surface of IgG. In addition, it was found that the replacement of the thioether sulfur atom with either a nitrogen or oxygen atom seems to have little influence on the binding of the ligand. Furthermore, the departing of MEP ligands from the surface of Fc-A at low pH was verified with the molecular simulation, mainly due to electrostatic repulsion. The MEP−DVS ligands with a sulfone group on the spacer arm would weaken the electrostatic repulsion and need more acidic

dx.doi.org/10.1021/jp206817b | J. Phys. Chem. B 2012, 116, 1393−1400

conditions for the departing. The results demonstrated that the molecular simulations would be helpful for better understanding the molecular mechanism of HCIC and improve the design of new ligands for antibody separation. Because of the limitation of the simplified ligand model used in the present work, the immobilized ligands on the support matrix will be studied in the coming future to obtain more detailed information on the protein−ligand support system.

■ ASSOCIATED CONTENT

Supporting Information

Force field parameters for six ligands tested, the possible binding sites of MEP−AB on Fc-A, the interaction energies for the ligands with the replacement of thioether sulfur of ligand, and the distance between MEP−AB and Fc-A during the simulation at two pH values. This material is available free of charge via the Internet at http://pubs.acs.org.

■ AUTHOR INFORMATION

Corresponding Author

*Tel/Fax: +86-571-87951982. E-mail: lindq@zju.edu.cn.

■ ACKNOWLEDGMENTS

This work was supported by the National Natural Science Foundation of China, the Program for New Century Excellent Talents in University (NCET), and the Fundamental Research Funds for the Central Universities.

■ REFERENCES

(1) Roque, A. C.; Lowe, C. R.; Taipa, M. A. *Biotechnol. Prog.* **2004**, *20*, 639−654.
(2) Reichert, J. M.; Rosensweig, C. J.; Faden, L. B.; Dewitz, M. C. *Nat. Biotechnol.* **2005**, *23*, 1073−1078.
(3) Kelley, B. *Biotechnol. Prog.* **2007**, *23*, 995−1008.
(4) Low, D.; O'Leary, R.; Pujar, N. S. *J. Chromatogr., B* **2007**, *848*, 48−63.
(5) Roque, A. C. A.; Silva, C. S. O.; Taipa, M. A. *J. Chromatogr., A* **2007**, *1160*, 44−55.
(6) Swinnen, K.; Krul, A.; Van Goidsenhoven, I.; Van Tichelt, N.; Roosen, A.; Van Houdt, K. *J .Chromatogr., B* **2007**, *848*, 97−107.
(7) Carter-Franklin, J. N.; Victa, C.; McDonald, P.; Fahrner, R. *J. Chromatogr., A* **2007**, *1163*, 105−111.
(8) Fassina, G.; Ruvo, M.; Palombo, G.; Verdoliva, A.; Marino, M. *J. Biochem. Biophys. Methods* **2001**, *49*, 481−490.
(9) Burton, S. C.; Harding, D. R. *J. Chromatogr., A* **1998**, *814*, 71−81.
(10) Boschetti, E. *Trends Biotechnol.* **2002**, *20*, 333−337.
(11) Guerrier, L.; Girot, P.; Schwartz, W.; Boschetti, E. *Bioseparation* **2000**, *9*, 211−221.
(12) Guerrier, L.; Flayeux, I.; Boschetti, E. *J. Chromatogr., B* **2001**, *755*, 37−46.
(13) Schwartz, W.; Judd, D.; Wysocki, M.; Guerrier, L.; Birck-Wilson, E.; Boschetti, E. *J. Chromatogr., A* **2001**, *908*, 251−263.
(14) Pujadas, G.; Vaque, M.; Ardevol, A.; Blade, C.; Salvado, M.; Blay, M.; Fernandez-Larrea, J.; Arola, L. *Curr. Pharm. Anal.* **2008**, *4*, 1−19.
(15) Adcock, S. A.; McCammon, J. A. *Chem. Rev.* **2006**, *106*, 1589−1615.
(16) Gilson, M. K.; Zhou, H. X. *Annu. Rev. Biophys. Biomol. Struct.* **2007**, *36*, 21−42.
(17) Zamolo, L.; Busini, V.; Moiani, D.; Moscatelli, D.; Cavallotti, C. *Biotechnol. Prog.* **2008**, *24*, 527−539.
(18) Boi, C.; Busini, V.; Salvalaglio, M.; Cavallotti, C.; Sarti, G. C. *J. Chromatogr., A* **2009**, *1216*, 8687−8696.
(19) Salvalaglio, M.; Zamolo, L.; Busini, V.; Moscatelli, D.; Cavallotti, C. *J. Chromatogr., A* **2009**, *1216*, 8678−8686.
(20) Zhang, L.; Zhao, G.; Sun, Y. *J. Phys. Chem. B* **2009**, *113*, 6873−6880.
(21) Zhang, L.; Sun, Y. *J. Biosci. Bioeng.* **2009**, *108*, S63−S63.
(22) Zhang, L.; Bai, S.; Sun, Y. *J. Mol. Graph. Model.* **2010**, *28*, 863−869.
(23) Zhang, L.; Zhao, G.; Sun, Y. *J. Phys. Chem. B* **2010**, *114*, 2203−2211.
(24) Wang, H. Y.; Lin, D. Q.; Yao, S. J.; Yuan, J. X.; Yao, K. J. *Acta Chim. Sin.* **2010**, *68*, 1597−1602.
(25) Burton, S.; Harding, D. *J. Chromatogr., A* **1998**, *796*, 273−282.
(26) Xia, H. F.; Lin, D. Q.; Wang, L. P.; Chen, Z. J.; Yao, S. J. *Ind. Eng. Chem. Res.* **2008**, *47*, 9566−9572.
(27) Boschetti, E. *J. Biochem. Biophys. Methods* **2001**, *49*, 361.
(28) Deisenhofer, J. *Biochemistry* **1981**, *20*, 2361−2370.
(29) Spassov, V. Z.; Yan, L. *Protein Sci.* **2008**, *17*, 1955−1970.
(30) Rocchia, W.; Alexov, E.; Honig, B. *J. Phys. Chem. B* **2001**, *105*, 6507−6514.
(31) Rocchia, W.; Sridharan, S.; Nicholls, A.; Alexov, E.; Chiabrera, A.; Honig, B. *J. Comput. Chem.* **2002**, *23*, 128−137.
(32) Delano, W. L.; Ultsch, M. H.; de Vos, A. M.; Wells, J. A. *Science* **2000**, *287*, 1279−1282.
(33) Diller, D. J.; Merz, K. M. Jr. *Proteins* **2001**, *43*, 113−124.
(34) Tirado-Rives, J.; Jorgensen, W. L. *J. Med. Chem.* **2006**, *49*, 5880−5884.
(35) Ryckaert, J. P.; Ciccotti, G.; Berendsen, H. J. C. *J. Comput. Phys.* **1977**, *23*, 327−341.
(36) Pettersen, E. F.; Goddard, T. D.; Huang, C. C.; Couch, G. S.; Greenblatt, D. M.; Meng, E. C.; Ferrin, T. E. *J. Comput. Chem.* **2004**, *25*, 1605−1612.
(37) Humphrey, W.; Dalke, A.; Schulten, K. *J. Mol. Graphics* **1996**, *14* (33−38), 27−38.
(38) Porath, J.; Hutchens, T. W. *Int. J. Quantum Chem.* **1987**, *32*, 297−315.
(39) Hutchens, T. W.; Porath, J. *Biochemistry* **1987**, *26*, 7199−7204.
(40) Berna, P. P.; Berna, N.; Porath, J.; Oscarsson, S. *J. Chromatogr., A* **1998**, *800*, 151−159.